International Communications in Heat and Mass Transfer 85 (2017) 139–146

Contents lists available at ScienceDirect

International Communications in Heat and Mass Transfer

journal homepage: www.elsevier.com/locate/ichmt

Mass transfer performance of the LiCl solution dehumidification process

Chunli Tang[a,b], Kambiz Vafai[b,*], Donghui Zhang[a]

[a] School of Energy and Power, Jiangsu University of Science and Technology, Zhenjiang 212003, China
[b] Mechanical Engineering Department, University of California, Riverside, CA 92521, USA

ARTICLE INFO

Keywords:
Driving force
Equilibrium curves
Overall volumetric mass transfer coefficient
Temperature variation

ABSTRACT

The driving force of the solution dehumidification process is investigated in this work, in which the parameters without the solute are used. The isothermal and non-isothermal equilibrium curves under some thermal conditions are calculated for the dehumidification process related to the LiCl solution as desiccant. Experiments based on the obtained equilibrium curves were performed for the structured packing tower with a height of 0.2 m and 0.3 m respectively. The temperature variation for the solution decreased with an increase in the solution flow rate and increased with an increasing airflow rate. But the temperature variation for the air did not display a marked trend. The average driving force and the overall mass transfer coefficients are calculated. The average driving force is investigated for different solution flow rates. The overall volumetric mass transfer coefficient increased with an increasing solution flow rate.

1. Introduction

For a traditional air conditioning system, the latent load may be handled by reducing the thermostat set-point well below the dew-point temperature to increase the condensation. As such, the air is reheated to bring the temperature back to the required value. This air-handling process is energy-inefficient [1]. Liquid desiccant dehumidification system reduces the water vapor content in moist air by means of the water vapor pressure difference between the moist air and the desiccant [2]. This is an efficient way to avoid the overcool/reheat scheme in the traditional air-handling process.

The characteristic of desiccants has a decisive effect on the system performance. The triethylene glycol (TEG) was used as a desiccant during the earlier times. It was then replaced by some salt solutions due to its high viscosity and volatility. McNeeley [3] and Kaita [4] tested the thermophysical properties of LiBr at different temperatures and concentrations. Liu et al. [5] summarized the features of LiBr and LiCl and experimentally compared their dehumidification performance, indicating LiCl solution was better than LiBr solution in the dehumidification process. Gong et al. [6] and Li et al. [7] tested the mixed solution of $CaCl_2$ and LiCl and investigated its dehumidification capacity. Conde [8] summarized the main parameters of $CaCl_2$ and LiCl and provided the relationship between such parameters as relative vapor pressure, density, viscosity, temperature and the desiccant mass concentration, which is important for the dehumidification applications.

Some of the relevant research works about the theoretical and experimental performance of different types of dehumidifiers are addressed here. Chen et al. [9] presented the mathematical models of an adiabatic dehumidifier, by applying the efficiency-heat transfer element method, and calculated the outlet parameters under several initial conditions. Dai and Zhang [10] and Khan and Sulsona [11] utilized a number of simplified models for cross-flow dehumidifiers and investigated the relationship between the relevant parameters. Liu et al. [12] and Gao et al. [13] established a cross-flow dehumidifier experimental setup and analyzed the influence of the inlet parameters on the dehumidifying performance. Zhang et al. [14] also investigated the dehumidifying performance of cross-flow dehumidifiers by using several different desiccants. In order to improve the overall system performance, the liquid desiccant dehumidification system was also coupled with such cooling systems as the vapor absorption system [15], cogeneration system [16] and heat pump system [17].

Counter-flow dehumidifier has a better performance in comparison with downstream and cross-flow type. Ren et al. [18,19] utilized a one-dimensional mathematical model of an adiabatic dehumidifier to analyze the coupled heat and mass transfer process. Li et al. [20] carried out a counter-flow dehumidifying experiment, by using $CaCl_2$ as a desiccant, and analyzed the influence of the solution flow and concentration on the outlet humidity of the air. Gu et al. [21] and Liu et al. [22] performed a similar set of experiments using LiCl as a desiccant. Babakhani and Soleymani [23] found a mathematical relationship between the dehumidification effectiveness and the mass transfer unit, and compared the results with some experimental data. Gandhidasan [24] obtained a correlation for the dehumidification

* Corresponding author.
E-mail address: vafai@engr.ucr.edu (K. Vafai).

http://dx.doi.org/10.1016/j.icheatmasstransfer.2017.04.013

Available online 26 May 2017

Nomenclature

a	specific surface area ($m^2 \cdot m^{-3}$)
d	air humidity ratio ($kg_{H2O} \cdot kg_{DA}^{-1}$)
h	specific enthalpy ($kJ \cdot kg^{-1}$)
k	single phase mass transfer coefficient ($kg \cdot m^{-2} \cdot s^{-1}$)
K	overall mass transfer coefficient ($kg \cdot m^{-2} \cdot s^{-1}$)
m	mass flow rate ($kg \cdot s^{-1}$)
M	mass flow rate without solute ($kg \cdot s^{-1}$)
N	mass flux rate ($kg \cdot m^{-2} \cdot s^{-1}$)
p	pressure (Pa)
Q	energy change rate (kW)
x	mass concentration of water in the liquid phase ($kg_{H2O} \cdot kg_l^{-1}$)
X	mass concentration without water solute in the liquid phase ($kg_{H2O} \cdot kg_{Licl}^{-1}$)
y	mass concentration of water in the gas phase ($kg_{H2O} \cdot kg_g^{-1}$)
Y	mass concentration without water solute in the gas phase ($kg_{H2O} \cdot kg_{DA}^{-1}$)
ΔY	the average driving force based on the mass concentration without the solute ($kg_{H2O} \cdot kg_{DA}^{-1}$)

Greek symbols

ε	mass concentration of LiCl in the solution
π	relative vapor pressure of the solution
ρ	density ($kg \cdot m^{-3}$)
φ	relative humidity (%)

Subscripts

DA	dry air
e	equilibrium status
g	air/gas
H_2O	water
i	inlet
l	liquid/solution
m	average
o	outlet
V	vapor

capacity under some inlet and outlet conditions. To improve the heat and mass transfer performance of the desiccant, Ali et al. [25–27] studied the dehumidification process by adding nanoparticle suspensions into the desiccant for different configurations. Their simulation results established that nanoparticles had a significant effect on improving the dehumidification process.

Prior works have mainly focused on the relationship between the macro parameters for the solution and the air. Relatively little attention has been given to the mass transfer driving force in the dehumidification process. The fitting curves based on the experimental data are discrete and non-universal. The equilibrium curves on the basis of equilibrium states are universal and can be used to design a dehumidification experiment and to analyze the mass transfer driving force.

In this work, the dehumidification process is analyzed while accounting for the mass transfer. The equilibrium curves for the dehumidification process using LiCl as the desiccant and the driving force based on these curves are obtained. The temperature variation for the solution and the air and the overall volumetric mass transfer coefficient based on the solution and moist air mass flow rate while carrying out LiCl solution dehumidification experiments are also analyzed. Our work can improve and enhance the dehumidification technology for air conditioning applications.

2. Mass transfer analysis for solution dehumidification

When the vapor pressure of an aqueous solution is less than the partial pressure of the water vapor of the moist air, the water vapor can transfer from the moist air to the solution. The greater the pressure difference, the higher the transfer rate for the water vapor. The parameters for the counter flow dehumidification process are shown in Fig. 1 [28].

Here z_1 and z_2 are the bottom and top position of the dehumidifier; m_{l1} and m_{l2} are the mass flow rate of liquid phase L with x_1 and x_2 being the corresponding mass concentration of water in the liquid phase. Similarly, m_{g1} and m_{g2} are the mass flow rate of gas phase G with y_1 and y_2 being the corresponding mass concentration of water vapor in the gas phase.

2.1.1. Mass transfer equation

Without chemical reaction, the mass balance equation of water in counter flow dehumidification process can be written as [28]:

$$m_{g1}y_1 + m_{l2}x_2 = m_{g2}y_2 + m_{l1}x_1 \tag{1}$$

The parameters without solute are used for simplifying the equations. So the mass concentrations without solute are written as

$$Y = \frac{y}{1-y} \tag{2a}$$

$$X = \frac{x}{1-x} \tag{2b}$$

The mass flow rate without solute can be written as

$$M_l = m_l \cdot (1-x) \tag{3a}$$

$$M_g = m_g \cdot (1-y) \tag{3b}$$

Substituting Eqs. (2a), (2b), (3a), and (3b) into Eq. (1), we obtain the following mass balance equation for water.

$$M_g Y_1 + M_l X_2 = M_g Y_2 + M_l X_1 \tag{4a}$$

$$\frac{M_l}{M_g} = \frac{Y_1 - Y_2}{X_1 - X_2} \tag{4b}$$

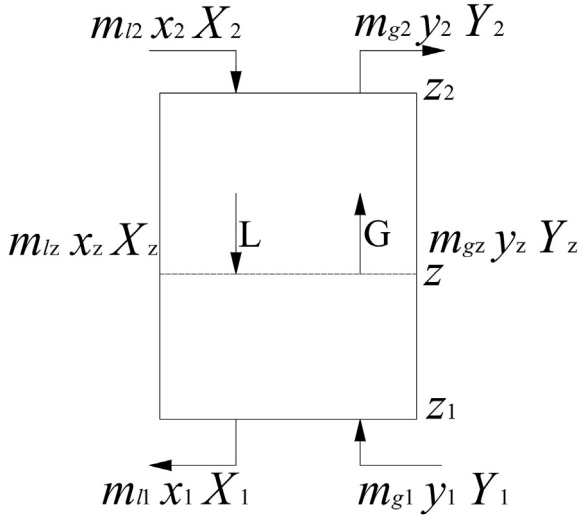

Fig. 1. Pertinent parameters for the counter flow dehumidification process.

Eq. (4b) is a straight line through two points of $(X_1,Y_1)$and(X_2,Y_2). It is called the operating line of mass transfer process for a counter flow.

2.1.2. Energy balance for the dehumidification process

The dehumidification process is accompanied by an energy exchange. The energy exchange in moist air and the solution can be written as:

$$\Delta Q_g = m_{g1}\cdot h_{g1} - m_{g2}\cdot h_{g2} \tag{5a}$$

$$\Delta Q_l = m_{l1}\cdot h_{l1} - m_{l2}\cdot h_{l2} \tag{5b}$$

Here ΔQ_g and ΔQ_l are the energy exchange rates for the air and the solution respectively, and h_{g1} and h_{g2} are the inlet and outlet specific enthalpies of the air, and h_{l2} and h_{l1} are the inlet and outlet specific enthalpies of the solution.

For an adiabatic device,

$$\Delta Q_l = \Delta Q_g \tag{6}$$

2.2. Properties of the two phases

2.2.1. Properties of the moist air

There are many parameters which describe the state of the moist air, such as the dry-bulb temperature (t), humidity (d), relative humidity (φ), and the partial pressure of the water vapor (p_V) etc. The one-to-one correspondence relationship between d and p_V can be described as

$$d = 0.622\cdot\frac{p_V}{p - p_V} \tag{7}$$

Here p_V is the partial vapor pressure of the bulk fluid and p is the atmospheric pressure.

2.2.2. Properties of LiCl solution

LiCl solution with lower surface vapor pressure is utilized as the desiccant. There are several parameters which specify the state of the solution, such as the temperature, density, concentration, vapor pressure, and specific thermal capacity etc. Conde [8] has provided a general relationship between the relative vapor pressure of the LiCl solution and the temperature and mass concentration as

$$\pi = \frac{p_l(\varepsilon, T)}{p_{H_2O}(T)} \tag{8}$$

Here $p_l(\varepsilon, T)$ is the vapor pressure of LiCl solution, and $p_{H_2}O(T)$ is the vapor pressure of the liquid water at a given temperature.

2.3. Equilibrium curves for the LiCl solution dehumidification process

The mass balance equation without solute can be useful when it is combined with the equilibrium curves. Therefore, in this work we have calculated the mass transfer equilibrium curves for the moist air and LiCl solution based on the equivalent vapor pressure within the two phases.

Dehumidification is typically an exothermic process. If the influence of latent heat on the temperature of the two phases can be ignored, their temperatures can be considered to be constant. The equilibrium curves which can be referred to as isothermal mass transfer are shown in Fig. 2a. Due to the latent heat, the temperature of the air and the solution change continuously during the dehumidification process. It is difficult to determine the proportion of the energy absorbed by the solution and the air. So it is assumed that all of the latent heat is absorbed by LiCl solution resulting in a temperature increase. This assumption is reasonable when the air temperature is close to or higher than the solution temperature. The equilibrium curves for variable temperature mass transfer are shown in Fig. 2b.

The ratio of water in moist air is less than that in LiCl solution but the effect of the change of the amount of water in moist air on its partial pressure is greater than the effect of the change of the amount of water in LiCl solution on its surface vapor pressure. Fig. 2a and b show that the change of water vapor partial pressure in moist air is greater than the change of vapor pressure on solution surface for the same amount of water. Therefore, the air flow rate can be increased to keep the same mass transfer driving force for the entire dehumidification process.

2.4. Dehumidification performance indices

Here, the mass transfer coefficient and the driving force for mass transfer are discussed in particular. The mass transfer rate per unit interface can be written as

$$N = K_g\cdot(p_g - p^*) \tag{9}$$

Here K_g is the gas-phase overall mass transfer coefficient [28,29], and p_g is partial pressure of water vapor in the bulk gas, p^* is the partial pressure of water vapor in the gas which is in equilibrium with the bulk liquid.

The specific surface area a is often used to calculate the mass transfer coefficient. The mass transfer rate can be written as

$$N\cdot a\cdot dz = K_g\cdot a\cdot(p_g - p^*)\cdot dz \tag{10}$$

Generally, the specific surface area a and the mass transfer coefficient are grouped together. This grouping determined by experiments, is referred to as overall volumetric mass transfer coefficient

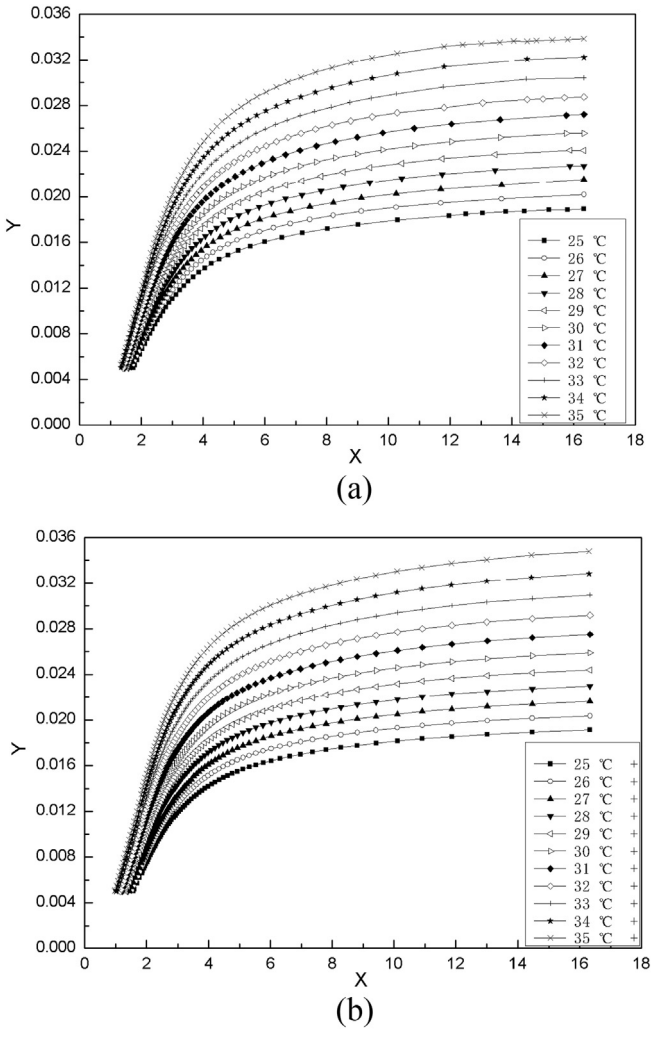

Fig. 2. Equilibrium curves for the mass transfer process for LiCl solution and moist air: (a) Isothermal case, (b) Non-isothermal case.

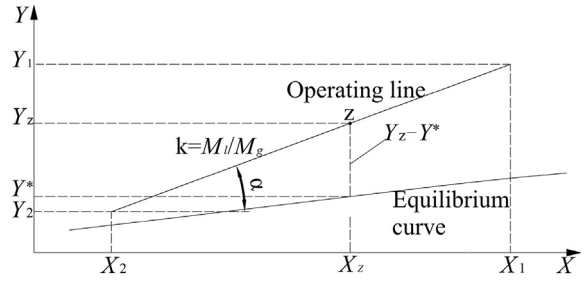

Fig. 3. The concentration driving force for the dehumidification process.

($K_g a$). Substituting the pressure driving force in Eq. (10) by the concentration driving force, the transferring quantity can be written as [29]:

$$N \cdot a \cdot dz = K_Y a \cdot (Y_z - Y^*) \cdot dz \tag{11}$$

Here Y^* is the equilibrium mass concentration without solute at position z as shown in Fig. 3.

Fig. 3 shows the relationship between the dehumidification process and the equilibrium curve when water transports from the gas phase to the liquid phase. Y_1 and Y_2 are the air mass concentrations without solute at the inlet and outlet, that is, the humidity ratio of the moist air and X_2 and X_1 are the solution mass concentrations without solute at the inlet and outlet. For an arbitrary position z, the mass concentrations without solute are X_z and Y_z in the liquid phase and gas phase respectively. $Y_z - Y^*$ is the driving force represented by the difference in mass concentrations without solute at position z, which exits only when the operating line is higher than the equilibrium curve.

The slope of the operating line in Fig. 3 is the ratio of mass flow rate without the solute. That is, the ratio of the mass of pure LiCl and the dry air. The change in the driving force can be decided by this ratio. Adjusting this ratio is helpful in analyzing the outlet air parameters.

3. Dehumidification experimental setup

The schematic diagram of a counter flow dehumidification system with LiCl as the liquid desiccant is shown in Fig. 4. The humid air, conditioned to the required temperature and humidity by using an air supply source, is blown into the dehumidifier from its bottom. The LiCl strong solution, cooled by the cooling water via a heat exchanger, goes through a rotameter and is pumped to the dehumidifier from its top. The air and solution go through the structured packing from opposite directions, where the heat and mass transfer take place. After absorbing the moisture from the air, the diluted solution flows into a reservoir.

Table 1
Specifications for different devices.

Parameters	Devices	Accuracy	Operational range
Air dry-bulb temperature	Thermocouple	± 0.1 °C	0–1600 °C
Air wet-bulb temperature	Thermocouple	± 0.1 °C	0–1600 °C
Air flow velocity	Hot-wire anemometer	± 0.1 m·s^{-1}	0–20 m·s^{-1}
Desiccant temperature	PT100	± 0.1 °C	− 200–420 °C
Desiccant volume flow rate	Rotameter	± 2.5%	25–1000 L·h − 1

Table 2
Initial values for the dehumidification experiments for 0.2 m height packing tower.

NO.	$t_{l,2}$ °C	$\varepsilon_{l,2}$	$m_{l,2}$ kg·s^{-1}	$t_{g,1}$ °C	$d_{g,1}$ × 10^3 kg·kg$_{DA}^{-1}$	$m_{g,1}$ kg·s^{-1}
1	30.97	0.324	0.067	30.76	22.215	0.035
2	29.24	0.320	0.067	28.07	20.328	0.050
3	30.72	0.326	0.067	31.34	23.508	0.065
4	32.17	0.323	0.102	30.76	22.374	0.035
5	30.59	0.319	0.102	28.23	20.289	0.050
6	30.96	0.328	0.102	31.26	23.470	0.065
7	30.87	0.322	0.133	31.26	22.862	0.035
8	30.41	0.319	0.133	28.32	20.437	0.050
9	30.50	0.329	0.133	31.19	23.479	0.065
10	31.20	0.321	0.166	31.11	23.519	0.035
11	30.38	0.320	0.166	28.36	20.838	0.050
12	30.58	0.330	0.166	31.83	22.188	0.065

Dehumidifier is the core device of the system, which is considered to be operating under adiabatic conditions during the experiment. The anti-corrosive pumps and PP-R pipes are used to transport the solution. Celdek structured packing with a 0.365 m width and a 0.365 m thickness, is used for heat and mass transfer with a large surface area density of 396 m^2·m^{-3}. Two packing heights of 0.2 m and 0.3 m are designed in order to find the influence of the packing height on the dehumidification performance. The diameter of the spray hole is 2 mm with 12 mm distance.

The operating parameters of moist air and LiCl solution are measured before and after the dehumidifier. The tested air parameters include the dry-bulb and wet-bulb temperatures, and the air velocity. The temperature is measured by a sensor installed in the air pipe, connected to a data acquisition instrument with a recording interval of 20s. The air mass flow is designed at 0.035 kg·s^{-1}, 0.050 kg·s^{-1} and

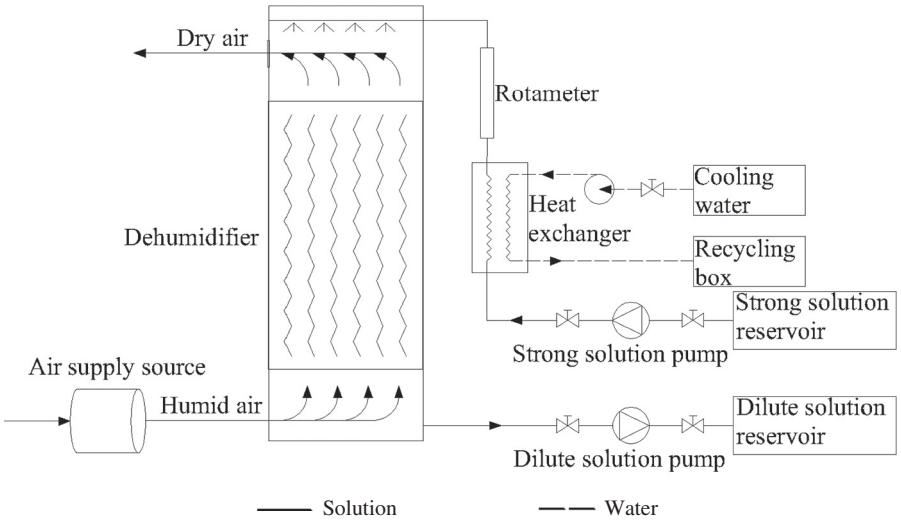

Fig. 4. Schematic diagram for the dehumidification experimental system.

Table 3
Initial values for the dehumidification experiments for 0.3 m height packing tower.

NO.	$t_{l,2}$ °C	$\varepsilon_{l,2}$	$m_{l,2}$ kg·s^{-1}	$t_{g,1}$ °C	$d_{g,1}$ × 10^3 kg·kg$_{DA}^{-1}$	$m_{g,1}$ kg·s^{-1}
1	31.73	0.343	0.067	31.83	27.762	0.035
2	31.91	0.351	0.067	31.70	29.554	0.050
3	31.46	0.337	0.067	32.94	29.986	0.065
4	31.06	0.350	0.102	31.61	28.108	0.035
5	31.99	0.355	0.102	30.11	26.191	0.050
6	31.86	0.334	0.102	34.02	31.415	0.065
7	31.50	0.348	0.133	32.51	28.883	0.035
8	31.83	0.357	0.133	31.97	28.157	0.050
9	32.13	0.332	0.133	34.14	31.826	0.065
10	31.74	0.347	0.166	32.56	28.011	0.035
11	31.00	0.362	0.166	31.76	27.398	0.050
12	32.15	0.330	0.166	34.09	31.781	0.065

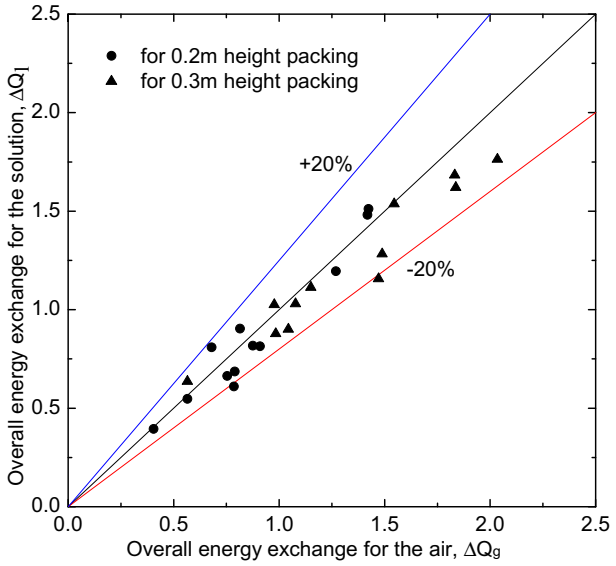

Fig. 5. Variation of the energy exchange in LiCl solution and the moist air.

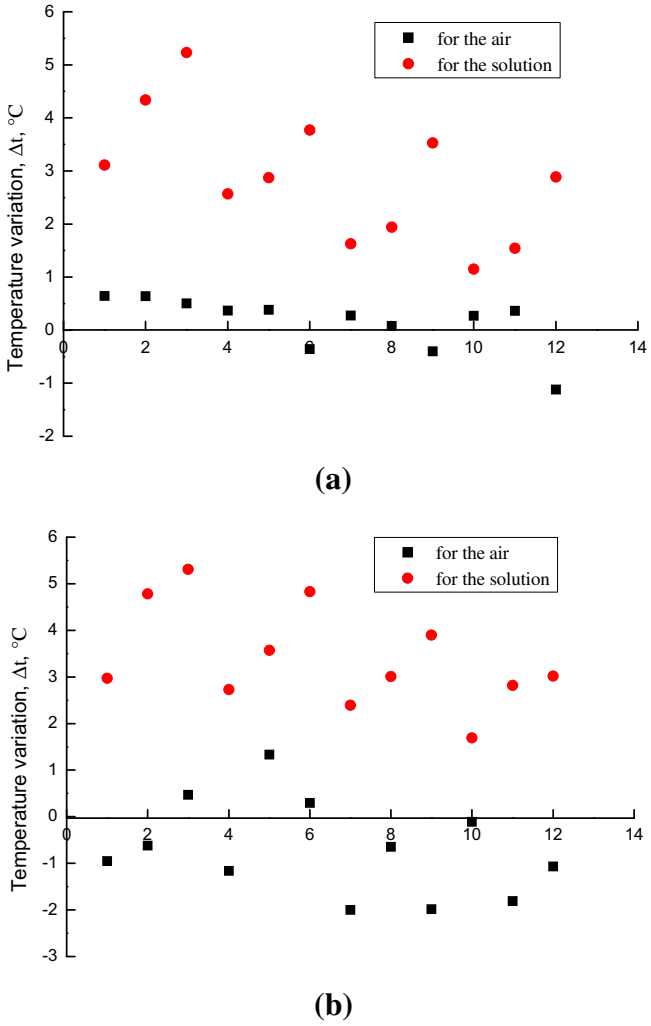

Fig. 6. Temperature variation for the air and the solution: (a) for a 0.2 m height packing, (b) for a 0.3 m height packing.

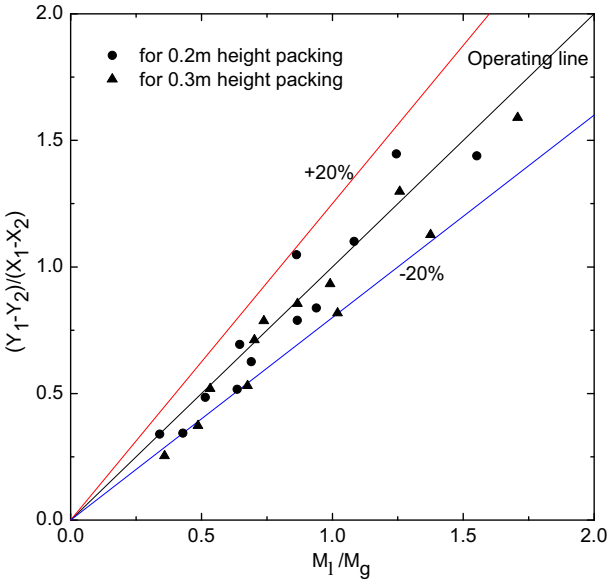

Fig. 7. Validation of the operating line equation by comparison with the experiments.

0.065 kg·s^{-1} respectively. It can be changed by the air velocity which is measured at 0.15 m distance away from the dehumidifier. The ultrasonic humidifier, installed at the inlet, is used to change the air humidity.

The tested LiCl solution parameters include the flow rate, temperature and the density. The solution flow rate can be adjusted by the valve installed next to the solution pump and measured by the rotameter installed before the dehumidifier. The solution sampling tube is installed at the inlet and outlet of the dehumidifier to take in a certain amount of the solution. The volume and mass are measured and the density is calculated. The concentration is obtained from the temperature-density-concentration chart. Specifications for the devices are shown in Table 1.

4. Experimental results and discussion

The initial values utilized in the dehumidification experiments for 0.2 m and 0.3 m height packing towers are shown in Tables 2 and 3 respectively.

4.1. Energy balance

The energy exchange is related to the temperatures, concentrations and flow rates. Fig. 5 shows that the energy balance between the air and the desiccant, obtained from Eqs. (5a) and (5b). The disagreement, by up to ± 20%, indicates the heat loss from the control volume to the

Table 4
Experimental data for the dehumidification process with 0.2 m height packing.

NO.	$t_{l,2}$ °C	X_2 $kg_{H2O}{\cdot}kg_{LiCl}^{-1}$	X_1 $kg_{H2O}{\cdot}kg_{LiCl}^{-1}$	$t_{g,1}$ °C	Y_1 $\times 10^3{\cdot}kg_{H2O}{\cdot}kg_{DA}^{-1}$	Y_2 $\times 10^3{\cdot}kg_{H2O}{\cdot}kg_{DA}^{-1}$	M_l/M_g	ΔY_m $\times 10^3{\cdot}kg_{H2O}{\cdot}kg_{DA}^{-1}$	K_Ya $kg{\cdot}m^{-3}{\cdot}s^{-1}$
1	30.97	2.09	2.099	30.76	22.215	17.56	0.632	9.035	0.661
2	29.24	2.15	2.164	28.07	20.328	15.678	0.429	6.82	1.217
3	30.72	2.068	2.082	31.34	23.508	18.931	0.340	10.24	1.063
4	32.17	2.099	2.108	30.76	22.374	14.836	0.939	7.079	1.269
5	30.59	2.14	2.15	28.23	20.289	13.35	0.646	6.376	2.075
6	30.96	2.053	2.068	31.26	23.47	16.189	0.515	9.029	1.923
7	30.87	2.108	2.114	31.26	22.862	14.176	1.245	7.816	1.43
8	30.41	2.132	2.14	28.32	20.437	12.052	0.863	6.572	2.217
9	30.5	2.04	2.053	31.19	23.479	15.344	0.69	9.1	2.133
10	31.2	2.114	2.12	31.11	23.519	14.882	1.552	8.027	1.533
11	30.38	2.125	2.132	28.36	20.838	13.13	1.083	6.788	2.304
12	30.58	2.03	2.04	31.83	22.188	14.3	0.866	9.18	2.155

Table 5
Experimental data for the dehumidification process with 0.3 m height packing.

NO.	$t_{l,2}$ °C	$\times_2$ $kg_{H2O}{\cdot}kg_{LiCl}^{-1}$	$\times_1$ $kg_{H2O}{\cdot}kg_{LiCl}^{-1}$	$t_{g,1}$ °C	Y_1 $\times 10^3{\cdot}kg_{H2O}{\cdot}kg_{DA}^{-1}$	Y_2 $\times 10^3\ kg_{H2O}{\cdot}kg_{DA}^{-1}$	M_l/M_g	ΔY_m $\times 10^3\ kg_{H2O}{\cdot}kg_{DA}^{-1}$	K_Ya $kg{\cdot}m^{-3}{\cdot}s^{-1}$
1	31.73	1.916	1.931	31.83	27.762	19.797	0.676	13.731	0.495
2	31.91	1.849	1.874	31.7	29.554	20.236	0.487	14.662	0.69
3	31.46	1.966	1.99	32.94	29.986	21.485	0.359	14.851	1.006
4	31.06	1.857	1.872	31.61	28.108	15.833	1.02	12.11	0.868
5	31.99	1.815	1.831	30.11	26.191	13.597	0.738	11.351	1.102
6	31.86	1.99	2.015	34.02	31.415	18.44	0.533	13.419	1.434
7	31.5	1.872	1.884	32.51	28.883	15.362	1.375	12.346	1.088
8	31.83	1.801	1.814	31.97	28.157	16.031	0.991	13.169	1.144
9	32.13	2.015	2.033	34.14	31.826	19.016	0.702	13.735	1.479
10	31.74	1.886	1.894	32.56	28.011	15.283	1.708	11.814	1.193
11	31	1.762	1.772	31.76	27.398	14.416	1.257	12.615	1.161
12	32.15	2.033	2.048	34.09	31.781	18.958	0.867	13.603	1.498

ambient air.

The overall energy exchange for the 0.3 m height packing tower is greater than that for 0.2 m height packing because the dehumidification capacity of the former is more than that of the latter.

4.2. Temperature variation for the air and the solution

The water vapor condenses with a heat release in the dehumidification process, which leads to an increase in the sensible heat. Fig. 6 shows the temperature variation for the air and the solution. The numbers for the horizontal coordinate in Fig. 6(a) and (b) are consistent with the serial number in Tables 2 and 3 respectively. The temperature variation for the solution decreases with an increase in the solution mass flow rate and increases with an increase in the air mass flow rate. But the temperature variation for the air does not have the same trend. The inlet air temperatures are close to the solution temperatures, which results in the temperatures for both the air and the solution to stay within a certain range. The hypothesis for Fig. 2(b) is also proved to be reasonable based on the temperature variation for the air and the solution.

4.3. Validation of the operating line equation

Fig. 7 shows a comparison of the ratio of the differences for the mass concentration without solute at the inlet and outlet and the ratio of the mass flow rates without solute. The experimental results are within approximately ± 20%.

4.4. Overall volumetric mass transfer coefficient

It is necessary to analyze the driving force and the overall volumetric mass transfer coefficient to evaluate the dehumidification process properly. Tables 4 and 5 show the parameters used in the experiments. The average driving force (ΔY_m) is the arithmetic average value of the inlet and outlet driving force. The driving force at the inlet and outlet are set by the temperatures and concentrations of the two phases, and the corresponding state in the equilibrium curve.

The average driving force is determined by both the inlet and outlet parameters and the equilibrium curve. However, the outlet parameters are related to the flow rates. So the average driving force also changes with the flow rates. Fig. 8 shows the average driving force changes with the solution mass flow rate for different air flow rates. When the solution flow rate increases from 0.067 $kg{\cdot}s^{-1}$ to 0.102 $kg{\cdot}s^{-1}$, the average driving force decreases consistently. When the solution flow rate increases from 0.102 $kg{\cdot}s^{-1}$ to 0.166 $kg{\cdot}s^{-1}$, the average driving force does not change significantly.

Fig. 9 shows the overall volumetric mass transfer coefficient variations with the solution flow rate for different air flow rates. The overall volumetric mass transfer coefficient increases with an increase in the solution flow rate. But this increase trends to reduce gradually with an increase in the solution flow rate.

Comparing Figs. 8 and 9, we can see that the average driving force for the 0.3 m height packing is greater than that for the 0.2 m height packing in the experiments. But the overall volumetric mass transfer coefficient for the 0.3 m height packing is less than that for the 0.2 m height packing. Therefore, a taller packing tower does not translate into a higher mass transfer rate. The influence of the solution flow rate on the average driving force and the overall volumetric mass transfer coefficient is more remarkable than that of the air flow rate.

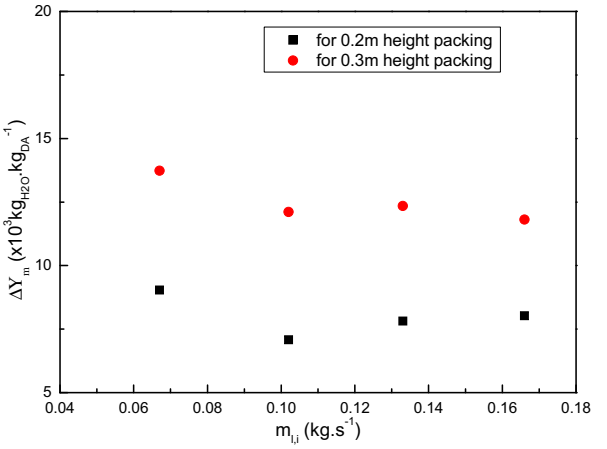

(a)

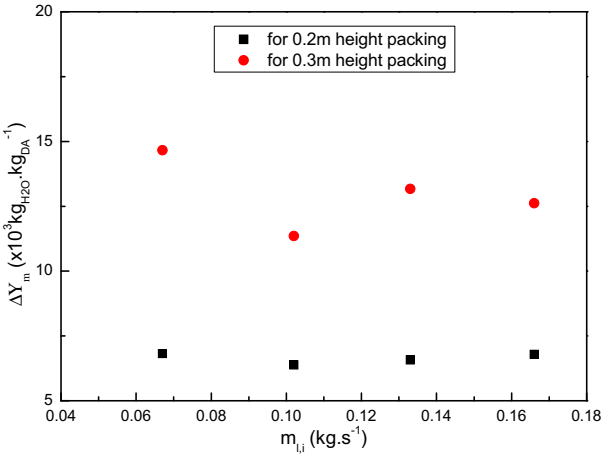

(b)

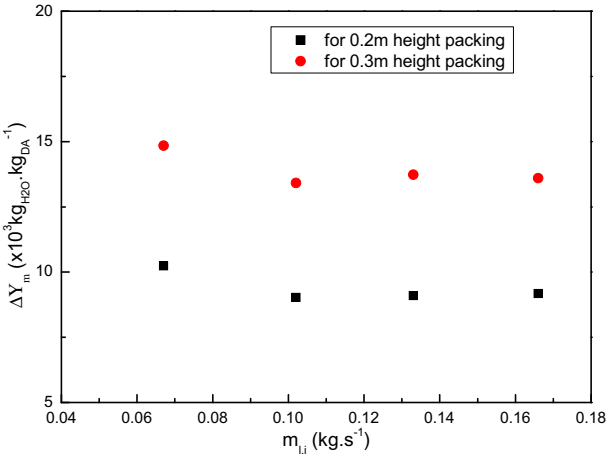

(c)

Fig. 8. Comparison of the average driving force for 0.2 m and 0.3 m height packing: (a) $m_{g,i}$ = 0.035 kg·s^{-1}, (b) $m_{g,i}$ = 0.05 kg·s^{-1}, (c) $m_{g,i}$ = 0.065 kg·s^{-1}.

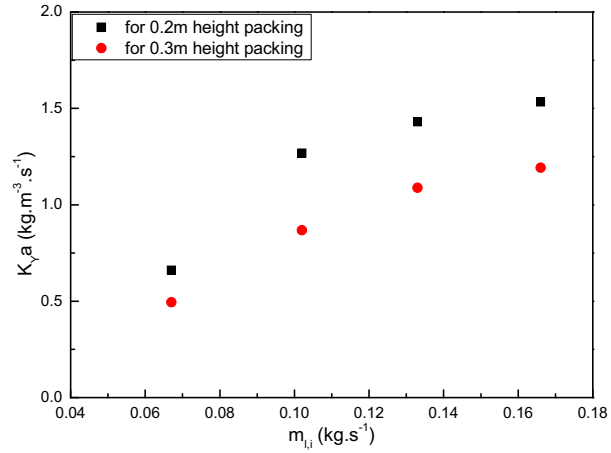

(a)

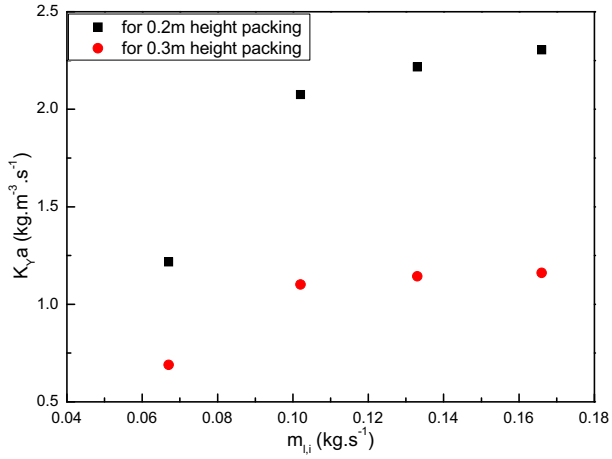

(b)

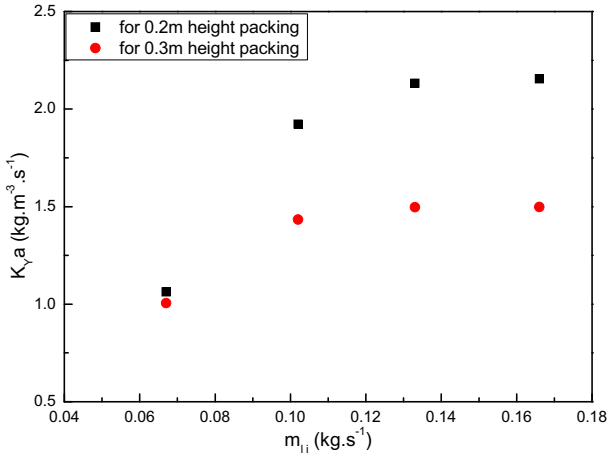

(c)

Fig. 9. Comparison of the overall volumetric mass transfer coefficient for 0.2 m and 0.3 m height packing: (a) $m_{g,i}$ = 0.035 kg·s^{-1}; (b) $m_{g,i}$ = 0.05 kg·s^{-1}; (c) $m_{g,i}$ = 0.065 kg·s^{-1}.

5. Conclusions

The mass transfer characteristics of the dehumidification process are analyzed in this study. The relationship of several parameters without solute is investigated. The equilibrium curves for the isothermal and non-isothermal mass transfer process based on the relationship for the parameters for the LiCl solution and the moist air are analyzed.

An experimental investigation is also carried out to verify the mass transfer equation without the solute to evaluate the performance of LiCl desiccant. The overall volumetric mass transfer coefficient is used as the performance indicator.

The solution temperatures change with an increase in the solution flow rate and the air flow rate with a distinct trend. However, the air

temperature does not follow a noticeable trend.

The average driving force varies differently within different solution flow rate range. The overall volumetric mass transfer coefficient increases with an increase in the solution flow rate. But this increasing trend reduces gradually with an increase in the solution flow rate. However, the influence of the air flow rate on the average driving force and the overall volumetric mass transfer coefficient is not noticeable.

The mass transfer equation without the solute was validated by comparison with the experimental data and a reasonable agreement between the experiments and the theory has been established. This study paves the way to utilize the mass transfer equation without solute to design the dehumidification process and to forecast the outlet parameters.

Acknowledgments

The authors are grateful for the financial support from the Foundation of Jiangsu Province through the Industry-University-Research Cooperation Prospect Project (no.BY2016073-10) and the Doctoral Foundation of Jiangsu University of Science and Technology (no.1142921505).

References

[1] T. Katejanekarn, S. Kumar, Performance of a solar-regenerated liquid desiccant ventilation pre-conditioning system, Energy Build. 40 (7) (2008) 1252–1267.
[2] D.G. Waugaman, A. Kini, C.F. Kettleborough, A review of desiccant cooling systems, Energy Resour. Technol. 115 (1993) 1–8.
[3] L.A. McNeeley, Thermodynamic properties of aqueous solutions of lithium bromide, ASHRAE Trans. 85 (2) (1979) 371–390.
[4] Y. Kaita, Thermodynamic properties of lithium bromide-water solutions at high temperatures, Int. J. Refrig. 24 (2001) 374–390.
[5] X.H. Liu, X.Q. Yi, Y. Jiang, Mass transfer performance comparison of two commonly used liquid desiccants: LiBr and LiCl aqueous solutions, Energy Convers. Manag. 52 (2011) 180–190.
[6] X.L. Gong, J. Sun, M.H. Shi, Contrast experimental study on performance of desiccation of desiccants solution, Refrig. Air Cond. 5 (5) (2005) 81–84.
[7] X.W. Li, X.S. Zhang, G. Wang, R.Q. Cao, Research on ratio selection of a mixed liquid desiccant: mixed LiCl–$CaCl_2$ solution, Sol. Energy 82 (2008) 1161–1171.
[8] M.R. Conde, Properties of aqueous solutions of lithium and calcium chlorides: formulations for use in air conditioning equipment design, Int. J. Therm. Sci. 43 (2004) 367–382.
[9] X.Y. Chen, Z. Li, Y. Jiang, Analytical solution of adiabatic heat and mass transfer process in packed-type liquid desiccant equipment and its application, Sol. Energy 80 (2006) 1509–1516.
[10] Y.J. Dai, H.F. Zhang, Numerical simulation and theoretical analysis of heat and mass transfer in a cross flow liquid desiccant air dehumidifier packed with honeycomb paper, Energy Convers. Manag. 45 (2004) 1343–1356.
[11] A.Y. Khan, F.J. Sulsona, Modeling and parametric analysis of heat and mass transfer performance of refrigerant cooled liquid desiccant absorbers, Int. J. Energy Res. 22 (9) (1998) 813–832.
[12] X.H. Liu, Y. Jiang, X.M. Chang, X.Q. Yi, Experimental investigation of the heat and mass transfer between air and liquid desiccant in a cross-flow regenerator, Renew. Energy 7 (2) (2006) 1–14.
[13] W.Z. Gao, J.H. Liu, Y.P. Cheng, X.L. Zhang, Experimental investigation on the heat and mass transfer between air and liquid desiccant in a cross-flow dehumidifier, Renew. Energy 37 (2012) 117–123.
[14] H.J. Zhang, J.H. Liu, L. Zhang, Experiment on mass transfer performance of a cross-flow dehumidifier, J. Refrig. 31 (6) (2010) 21–27.
[15] Q. Ma, R.Z. Wang, Y.J. Dai, X.Q. Zhai, Performance analysis on a hybrid air-conditioning system of a green building, Energy Build. 38 (5) (2006) 447–453.
[16] X.H. Liu, K.C. Geng, B.R. Lin, Y. Jiang, Combined cogeneration and liquid-desiccant system applied in a demonstration building, Energy Build. 36 (9) (2004) 945–953.
[17] C.K. Lee, H.N. Lam, Computer simulation of ground-coupled liquid desiccant air conditioner for sub-tropical regions, Int. J. Therm. Sci. 48 (12) (2009) 2365–2374.
[18] C.Q. Ren, Y. Jiang, G.F. Tang, Y.P. Zhang, A characteristic study of liquid desiccant dehumidification/regeneration processes, Sol. Energy 79 (2005) 483–494.
[19] C.Q. Ren, Y. Jiang, Y.P. Zhang, Simplified analysis of coupled heat and mass transfer processes in packed bed liquid desiccant-air contact system, Sol. Energy 80 (2006) 121–131.
[20] W.Y. Li, Y. Dong, C.C. Fang, The experimental research of liquid dehumidifying system, Acta Energiae Solaris Sin. 21 (4) (2000) 91–395.
[21] J. Gu, J.J. Wen, Z.C. Tian, Experimental research on dehumidifier using LiCl solution as liquid desiccant, Trans. CSAE 2 (3) (2006) 121–126.
[22] J.H. Liu, Z.M. Wu, Y.H. Ding, W.G. Gu, Study on the performance of dehumidifier in the liquid desiccant air conditioning system, Fluid Mach. 33 (12) (2005) 61–64.
[23] D. Babakhani, M. Soleymani, An analytical solution for air dehumidification by liquid desiccant in a packed column, Int. Commun. Heat Mass Transfer 36 (2009) 969–977.
[24] P. Gandhidasan, A simplified model for air dehumidification with liquid desiccant, Sol. Energy 76 (2004) 409–416.
[25] A. Ali, K. Vafai, A.-R.A. Khaled, Comparative study between parallel and counter flow configurations between air and falling film desiccant in the presence of nanoparticle suspensions, Int. J. Energy Res. 27 (2003) 725–745.
[26] A. Ali, K. Vafai, A.-R.A. Khaled, Analysis of heat and mass transfer between air and falling film in a cross flow configuration, Int. J. Heat Mass Transf. 47 (2004) 743–755.
[27] A. Ali, K. Vafai, An investigation of heat and mass transfer between air and desiccant film in an inclined parallel and counter flow channels, Int. J. Heat Mass Transf. 47 (2004) 1745–1760.
[28] J.R. Welty, C.E. Wicks, R.E. Wilson, G.L. Rorrer, Fundamentals of Momentum, Heat and Mass Transfer (the Fourth Edition), Chemical Industry Press, 2005.
[29] K. Asano, Mass Transfer from Fundamentals to Modern Industrial Applications, Wiley-VCH Verlag GmbH & Co. KGaA, Weinheim, Germany, 2006.